

FEATURED RESEARCH

Torsion of the Left Ventricle During Pacing with MRI Tagging

Jonathan M. Sorger, B.S.,^{1,2} Bradley T. Wyman, Ph.D.,¹ Owen P. Faris, Ph.D.,^{1,2}
William C. Hunter, Ph.D.,¹ and Elliot R. McVeigh, Ph.D.^{1,2,*}

¹Department of Biomedical Engineering, The Johns Hopkins University School of Medicine, Baltimore, Maryland, USA

²Laboratory of Cardiac Energetics, National Institutes of Health, National Heart, Lung and Blood Institute, Bethesda, Maryland, USA

ABSTRACT

The effects of different pacing protocols on left ventricular (LV) torsion were evaluated over the full cardiac cycle. A systolic and diastolic series of magnetic resonance imaging (MRI) scans were combined and used to calculate the torsion of the LV in a canine model. The asynchronous activation resulting from ventricular pacing interferes with the temporal evolution of LV torsion. The torsion of the left ventricle was investigated under three different protocols: 1) right atrial pacing, 2) right ventricular pacing, and 3) simultaneous pacing from the right ventricular apex and LV base. The temporal evolution of torsion was determined from tagged MRI and evaluated over the cardiac cycle. The peak rotation for the atrially paced hearts was $11.1^\circ (\pm 3.5^\circ)$ compared to $6.1^\circ (\pm 1.7^\circ)$ and $6.1^\circ (\pm 0.7^\circ)$ for those hearts paced from the right ventricle and from both ventricles, respectively. While biventricular pacing increases the synchrony of contraction, it significantly alters the pattern of LV torsion. From these experiments we have shown that measuring torsion is an extremely sensitive indicator of the existence of ectopic excitation.

Key Words: Cardiac; MRI; Pacing; Torsion; Ventricle.

INTRODUCTION

Left ventricular torsion is the relative rotation of the apex with respect to the base, and plays an important role

in the proper filling and ejection mechanics of the left ventricle (LV) (Robinson et al., 1986). During contraction, the apex of the LV rotates in a counterclockwise direction when viewed from apex to base. This rotation

*Correspondence: Elliot R. McVeigh, Ph.D., Laboratory of Cardiac Energetics, National Institutes of Health, National Heart, Lung and Blood Institute, 10 Center Drive, MSC-1061, Building 10, Room B1D416, Bethesda, MD 20892-1061, USA; Fax: (301) 402-2389; E-mail: emcveigh@bme.jhu.edu.



permits the endocardium to contract more than the epicardium, resulting in a greater ejection than would otherwise occur. In diastole, a rapid untwisting occurs before the rapid filling phase (Beyar et al., 1989; Rademakers et al., 1992), and is thought to release stored energy, augmenting LV filling. The purpose of this study was to determine the effects of asynchronous contraction and relaxation resulting from ectopic pacing on the rotational mechanics of the LV over the full cycle.

The untwisting phase has been shown to be a sensitive indicator in detecting changes in heart function. Studies have shown that small decreases in the rate of untwist during the diastolic phase are an early indicator of allograft rejection (Yun et al., 1991) and the onset of congestive heart failure (Ohno et al., 1994). Additionally, the rate of untwist has been shown to increase with inotropic stimulation (Rademakers et al., 1992). Also, increases in pressure during isovolumetric relaxation have been shown to be a predictor of a positive response to beta-adrenergic blocking agents in the treatment of dilated cardiomyopathy (Eichhorn et al., 1995). Thus, the ability to noninvasively detect changes in the dynamics of the torsion of the LV would have direct clinical implications. In this study we evaluate the effects of different pacing protocols on LV torsion during both systole and diastole.

Previously, researchers have investigated torsion of the heart using radiopaque markers and biplane cineradiography (Beyar et al., 1989; Ingels et al., 1975; Waldman et al., 1985; Yun et al., 1991) echocardiography (Arts et al., 1984), optical devices (Gibbons-Kroeker et al., 1995), and tagged MRI (Buchalter et al., 1994). Tagged MRI has been used to provide transmural torsion throughout the LV, but due to tag fading this method has only recently been used to analyze the full cardiac cycle (Stuber et al., 1999). In this study we overcome the tag fading problem and generate full-cycle data by splicing together a systolic and diastolic series of tagged images.

Investigating how different pacing protocols affect the twisting and untwisting of the ventricle can indicate which pacing protocols are able to best preserve the rotational mechanics of the LV and can perhaps lead to a better understanding of the causes of the twist. It is well established that pacing the heart from a ventricular site results in an asynchronous contraction of the LV (Badke et al., 1980; McVeigh et al., 1996; Wyman et al., 1999), which affects the diastolic phase of the heart as reflected by a reduction in the maximum decline in pressure during filling, dp/dt_{\min} (Bedotto et al., 1990). The role of torsion in this change of function is unknown.

In this study we demonstrate that the asynchronous contraction resulting from ventricular pacing alters the

temporal evolution of torsion of the LV. Torsion was analyzed under various pacing protocols to determine if increasing the synchrony of contraction with biventricular (Bi-V) pacing can preserve the torsional mechanics of the LV.

METHODS

In these experiments the canine heart was paced from each of three sites: right atrium (RA), apex of the right ventricle (RVa), and simultaneously from the LV freewall and RVa sites (Bi-V). During ventricular pacing the RA was paced simultaneously to override the intrinsic sinoatrial node excitation. A series of tagged MR images was acquired for systole and then diastole during each of the pacing protocols and processed to determine the temporal evolution of torsion, as well as the minimum and maximum angles of rotation.

Animal Preparation

Five mongrel dogs (weight 20–25 kg) were initially anesthetized with sodium pentothal (20 mg/kg), and then anesthesia was maintained with isoflourane (0.8–1.25%). Tygon catheters were inserted into the jugular vein and the femoral artery for fluid and drug administration, and an MR-compatible Millar catheter tip micro-manometer (model SPC-350MR, Millar Instruments Inc., Houston, TX) was inserted into the left ventricle via the carotid artery to monitor pressure. Under fluoroscopic guidance the RVa pacing catheter (Bard, Murray Hill, NJ) was inserted into the apex of the right ventricle via either the femoral or the jugular vein. After the chest was opened, nonferromagnetic bipolar pacing leads were sewn on the heart at the right atrium and the base of the left ventricular freewall. Two additional electrodes were attached to the RV and LV for electrical monitoring of the heart. Throughout the experiments the stability of the animal preparation was monitored with arterial blood pressure, as well as observation of the end-diastolic LV volume and ejection fraction as estimated from the MR images. After the experiment the animal was sacrificed with an overdose of pentobarbital. The experiments were performed with approval of the Johns Hopkins Animal Care and Use Committee.

Pacing Protocol

As previously described, the electrodes were filtered through a passive low-pass LC filter designed to attenuate signals at the operating frequency of the MRI



scanner (64 MHz) and at the frequencies induced by gradient switching (Tsitlik et al., 1992). After filtering, the pacing leads were passed outside the scanner room where they were simultaneously recorded on a Gould 4-channel recorder (TA240S, Gould Instruments, Valley View, OH) and sampled at 2000 Hz using a data acquisition card (PC1200, National Semiconductors, Austin, TX) and LabView software running on a Macintosh Power PC. The pressure information from the Millar catheter in the LV and the pacing signal were also recorded. Pacing was performed using a GRASS stimulator (S48, Grass Instruments, Quincy, MA) connected to an isolation stimulus unit (SIU5, Grass) for each of the pacing sites. The stimulus levels were independently set at a level high enough to ensure consistent capture as verified by ECG, LV pressure, and the CINE MR data. The normal electrical activation of the heart was suppressed by using A-V synchronous pacing at a rate above the spontaneous rate.

MRI Protocol

For each pacing protocol a cine series of MR images was acquired from both the systolic and diastolic phases of the heart cycle. The studies were performed on a GE SIGNA 1.5 T scanner (GE Medical Systems, Milwaukee, WI) using segmented *k*-space acquisitions during breath-hold periods (McVeigh, 1996; McVeigh and Atalar, 1992). Ten- to 20-second breath-holds were accomplished by stopping the ventilator at an identical point in the respiratory cycle. Each breath-hold was followed by a recovery period of 30–40 seconds. The tags were placed on the myocardium by saturating the proton spins in evenly spaced planes (Axel and Dougherty, 1989). When the images were subsequently taken perpendicular to the tag planes these tags were seen on the images as dark lines. The inverted proton spins moved with the heart and served as material point markers, which were used to determine the tissue displacements orthogonal to the tags (McVeigh, 1996; McVeigh and Zerhouni, 1991). The tagging pattern produced 1.5-mm thick saturation bands spaced at 5.5-mm intervals. The scanning parameters used were 28–32 cm field-of-view, TR of 3.2–4.4 ms, TE of 1.2 ms, 256 × 96 acquisition matrix, ± 32 kHz bandwidth, 5 readouts per movie frame, and in-plane spatial resolution of 1.25 mm × 3 mm and a slice thickness of 7 mm.

To image the motion of the tags during systole in the ventricularly paced experiments, the scanner was triggered by a pulse that preceded the pacing signal by 40 ms and resulted in tagging in late diastole before the onset of pacing. For the atrially paced experiments, tagging

occurred at late diastole as determined from the cine sequence of MR images, and imaging followed the atrioventricular delay. Fourteen to 18 images were acquired at 16–22 ms intervals with the first image occurring at 6 ms after tagging.

The diastolic images were acquired for four of the experiments by triggering the scanner at end-systole so that tagging took place at a time corresponding to one of the last images of the systolic acquisition. Fourteen to 18 images were then acquired at 16–22 ms intervals through diastole. In the fifth experiment, tagging occurred at end-diastole but imaging was delayed until end-systole. This modification yields higher contrast tags at end-systole and through diastolic relaxation due to the fact that the magnetization is not driven towards equilibrium during systole. When feasible, diastolic imaging continued through the start of systole so that the diastolic and systolic sets had an overlap of one or two images.

For each of the three pacing sites, seven to nine short-axis slices were acquired with a parallel line tagging pattern with the tags perpendicular to the frequency encoding direction, followed by the same set of short-axis slices with both the tags and readout gradient rotated 90° (McVeigh, 1996; McVeigh and Atalar, 1992). Nine long-axis slices with the slices oriented radially from the center of the LV cavity and spaced 20° apart were imaged with the tags parallel to the short-axis imaging planes. The complete acquisition took approximately 40–50 minutes.

Data Processing

The tagged MR images were analyzed by delineating the contours and the tags using a semiautomated software package (Guttman et al., 1994; 1997). The three-dimensional displacements were calculated by field-fitting the displacements in prolate spheroidal coordinates using the method described by O'Dell et al. (1995). Field-fitting uses the three orthogonal sets of one-dimensional displacements measured from the tags to generate an analytical solution of the three-dimensional displacement field, permitting the calculation of displacement at any location. A regularly spaced mesh of material points is defined at the first time frame. Then, using the tags to calculate a displacement field, the trajectory of the material points of the mesh was computed. The torsion was then calculated from the mesh. For this study a mesh of three radial shells, seven to nine longitudinal slices, and 24 circumferential points were used.



Torsion Calculation

The following definitions will be useful in this discussion: Rotation: θ_{base} , θ_{apex} ; Twist: $\theta_{\text{apex}} - \theta_{\text{base}}$; Torsion: $(\theta_{\text{apex}} - \theta_{\text{base}})/L$ where L is the distance from the center of the apical-most, short-axis slice to the center of the basal-most, short-axis slice. A regularly spaced mesh was used to define the location, or the material points used in the calculation of torsion. The undeformed parallel tags served as the reference state, and the deformed mesh represented the same myocardial locations as they moved throughout the cardiac cycle. The full three-dimensional data set was calculated using a mesh of three radial, seven or eight longitudinal, and 24 circumferential points. The mesh was defined at the first systolic imaging time frame with the longitudinal locations at the short-axis imaging plane levels. As the heart deformed, the mesh points within a slice were no longer coplanar and became oblique. A two-dimensional frame of reference with coplanar mesh slices was generated for calculating the angles of rotation. Each slice was centered using the centroid of the 24 circumferential mesh points. The Z position was calculated as the distance of that slice from the apical-most slice. With this frame of reference, the angles of rotation in the XY plane could easily be calculated. The direction of normal systolic torsion, or counterclockwise twist as viewed from the apex towards the base, was considered positive. Average rotations for each slice were calculated from the average of the 24 circumferential points, and regional twist was calculated in the septum, anterior, posterior, and lateral freewall by averaging the corresponding six circumferential points at those locations. The positive direction of rotation ($\theta > 0$) was defined as a counterclockwise rotation of the heart when viewed from apex to base.

RESULTS

Basal Slice Motion

Since the basal slice was used as the reference frame for all of the measurements, the absolute motion of this slice is considered independently. Figure 1 shows the basal rotation across all pacing protocols at the endocardium, midwall, and epicardium. The basal motion was predominantly in the clockwise direction when viewed from the apex during systole. The basal rotation was fairly consistent across pacing protocols with greater differences found among studies than among pacing protocols (data not shown). However, one study demonstrated minimal rotation across all pacing protocols. In general, hearts paced from the RA showed a greater degree of basal rotation than did hearts paced from other sites, and this rotation was always greater in the endocardium than in the midwall or epicardium.

Torsion by Slice

As expected, the rotation of each slice progressively increased towards the apex. The temporal evolution was similar across slices with the primary difference being that the amplitude increased as a function of distance from the base. This consistent progression of rotation and similarity in time course from one slice to the next was consistent across all hearts and across pacing protocols. Given this consistency, the second-most apical slice was used for detailed analysis since the apical-most slice was usually at the cap of the apex and was prone to increased noise from the prolate spheroidal field-fitting method.

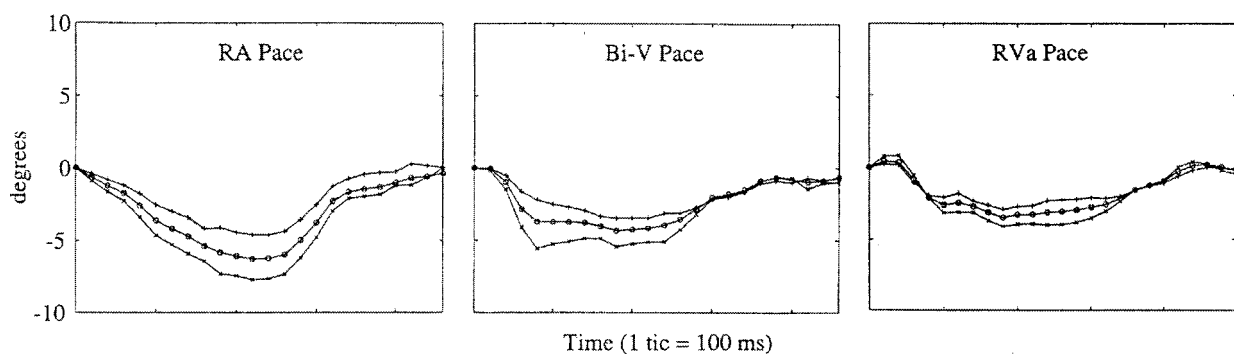


Figure 1. Basal rotation across all pacing protocols at the endocardium (\times), midwall (\circ), and epicardium ($+$). The basal motion was predominantly in the clockwise direction when viewed from the apex during systole.

Apical Torsion by Pacing Site

Figure 2 shows the twist of the endocardium, midwall, and epicardium at the apex of each heart for all of the pacing protocols. From the data a few generalizations can be made. First, the systolic rotation was positive (counterclockwise when viewed from the apex). Often there was a slight, initial, negative twist, which occurred at the time of the onset of contraction, and this initial twist was more prevalent in the paced experiments. The endocardium always demonstrated the largest rotation, while the epicardium always had the smallest rotation.

The shape of the temporal twist curves, shown in Fig. 2, was very consistent across animals within a pacing protocol. Right-atrium-paced hearts had a smooth progression of twist, which was, in most cases, nearly symmetric about the peak. From the initial reference (end-diastole) the rotation in the RA-paced hearts returned to the reference state without overshooting into negative angles. All of the ventricularly paced hearts took longer to reach peak torsion than the RA-paced hearts.

The Bi-V-paced hearts exhibited a double peak during systolic twist, which was then followed by an overshoot of untwisting before returning to the reference state at the end of the cycle as shown in Fig. 2. The maximum angle of rotation was generally smaller than that seen in RA pacing, though the negative untwisting often resulted in a larger peak-to-peak twisting amplitude than RA pacing. The RVa-paced hearts resembled the Bi-V-paced hearts in that they had a double peak during systole and an overshoot of the untwisting during diastole. This biphasic effect may be due to the fact that there was no delay between the pacing of the right atrium and the pacing of the ventricle(s).

Regional Variation

The regional differences in the LV were small, usually less than 2° , but in a few cases differences up to 5° were seen. The anterior wall consistently had a greater twist during systole than the other regions. Regional differences for a study are shown in Fig. 3.

Rotational Parameters

The averages of the maximum and minimum peak twists (T_{\max} and T_{\min}) of the endocardium are shown in Table 1 for all pacing protocols. The T_{\max} for the RA-paced experiments was always greater than the T_{\max} for the other pacing protocols. T_{\min} is the amount that the heart overshoot the reference state of zero twist, as shown in Fig. 2. Ventricularly paced hearts had a greater propensity for untwisting beyond the reference state.

To further quantify the differences between protocols, torsion vs. percent fill fraction was plotted, as shown in Fig. 4. Hearts are considered to be at 100% fill fraction at the beginning of systole and are at their lowest percent fill fraction at end-systole. The RA-paced experiments produce curves similar to those previously reported by Yun et al. (1991) for healthy hearts. However, pacing from ventricular sites disrupts the smooth, continuous evolution of twist, producing curves more rectangular in shape. In addition, the ventricularly paced hearts exhibit rapid isovolumic diastolic untwist when compared to those paced atrially. To illustrate the rapid untwist, the ratio of diastolic isovolumic torsion to systolic torsion was examined. The results are shown in Table 1, with the ratio being 0.5 ± 0.3 for the RA-paced hearts and tripling for those hearts paced biventricularly (1.9 ± 1.1) as well as from the right

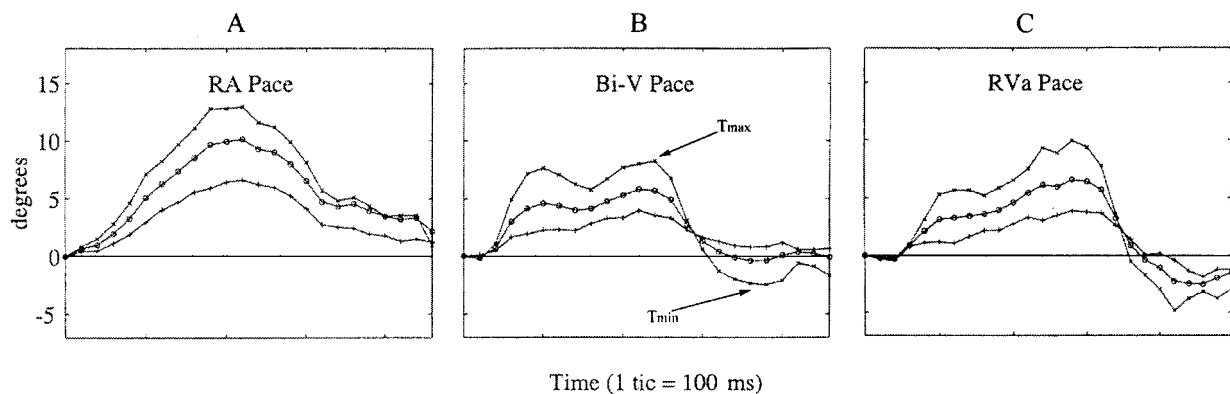


Figure 2. Rotation of the apical slice for the study shown in Fig. 1 for each pacing site. Rotation at the endocardium (\times), midwall (\circ), and epicardium ($+$) is shown.



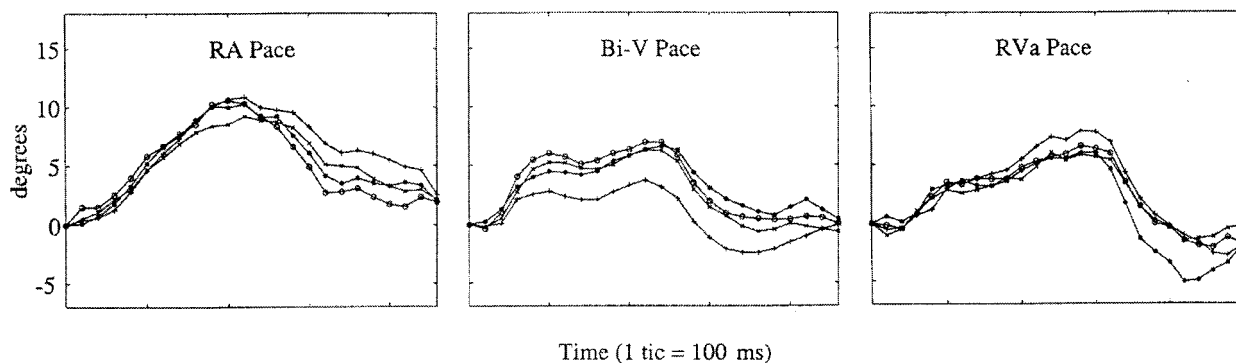


Figure 3. Regional rotation for the study shown in Fig. 1. Data is shown for septum (\times), anterior wall (\circ), lateral wall ($+$) and posterior wall ($*$).

ventricle (1.5 ± 0.5). This change in the ratio shows that on average, the RVa- and Bi-V-paced hearts exhibit a much greater amount of isovolumic untwist than the RA-paced hearts.

DISCUSSION

Summary of Results

In general, the base of the heart rotated in a clockwise direction while the apex rotated counterclockwise during systole with the net twist being in the counterclockwise direction. This direction of torsion was preserved during pacing from all sites; however, the ventricular pacing protocols reduced the amplitude of the peak twist, when compared to those hearts paced atrially. During diastolic untwisting the ventricularly paced hearts consistently overshoot the return to zero twist, resulting in a second small rotation at end-diastole. This overshoot may be responsible for reduced diastolic

efficiency, as the mechanics of contraction are obviously drastically altered through pacing. It is possible that due to the overshoot, reverse flow may have occurred during diastole. The regional differences in twist were mostly consistent across all pacing protocols, with the anterior wall having the greatest absolute magnitude. A significant result was that increasing the synchronization of contraction through Bi-V pacing (Wyman et al., 2002) did not restore the patterns of rotation seen in the RA-paced hearts.

Comparison with Other Results

The bulk rotation of the LV base in the clockwise direction during systole is consistent with the results of Ingels et al. (1975), who reported that the base and the apex rotated in opposite directions. This result, however, conflicts with the results of Gibbons-Kroeker et al. (1995) who reported that the rotation of the LV base was minimal. Though one heart in our studies showed

Table 1. Averages (\pm std dev.) for the parameters calculated from the endocardial twist data for all paired experiments ($n = 5$). T_{\max} and T_{\min} are the maximum and minimum angle of twist. P_{\max} is the maximum pressure and dP/dt_{\min} is the peak rate of pressure decline during diastole. Systolic torsion/isovolumic torsion is the ratio of the twist occurring during systole divided by the amount of untwist occurring during isovolumic relaxation.

	RA	Bi-V	RVa
T_{\max} ($^{\circ}$)	11.5 (\pm 3.1)	6.1 (\pm 0.7) ^a	6.1 (\pm 1.7) ^a
T_{\min} ($^{\circ}$)	-0.8 (\pm 1.1)	-4.5 (\pm 2.5) ^b	-4.8 (\pm 4.3)
P_{\max} (mm Hg)	87.5 (\pm 16.5)	88.9 (\pm 12.6)	79.4 (\pm 23.5)
dP/dt_{\min} (mm Hg/s)	-1.6 (\pm 0.9)	-1.5 (\pm 0.5)	-1.3 (\pm 0.9)
Systolic torsion/isovolumic torsion	0.5 (\pm 0.3)	1.9 (\pm 1.1) ^c	1.5 (\pm 0.5) ^c

^a T_{\max} for RVa and Bi-V pacing was significantly different than for RA pacing by the Student's t -test ($p < 0.01$).

^b T_{\min} for Bi-V pacing was significantly different than for RA pacing ($p < 0.05$).

^cSystolic twist/isovolumic untwist for RVa and Bi-V pacing was significantly different than for RA pacing ($p < 0.001$).

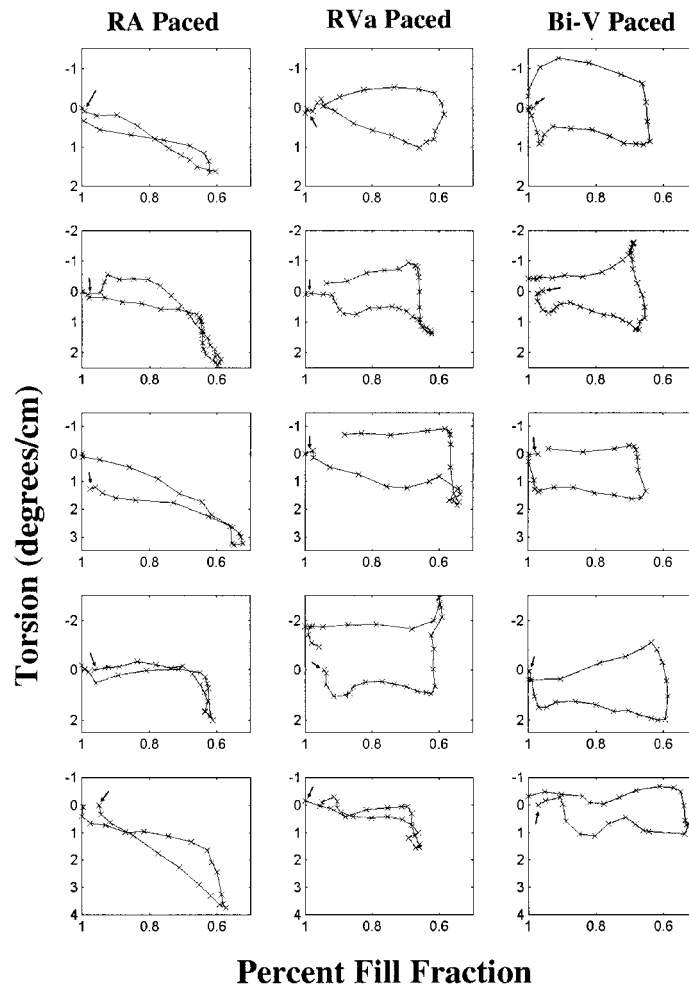


Figure 4. Torsion vs. percent fill fraction for all studies. Hearts are considered to be at 100% fill fraction at the beginning of systole and are at their lowest percent fill fraction at end-systole. Arrows denote the beginning of systole.

minimal basal rotation, the other four studies had significant clockwise rotation during contraction. To confirm that the rotation was not an artifact of the mathematical methods, the raw tagged images of the LV base were examined and the base clearly rotated in a clockwise direction. It is possible that the thoracotomy and disruption of the pericardium during surgery may have affected the direction and freedom of torsion in the heart. However, Rademakers et al. (1992) found that the peak torsion was the same in closed-chest dogs as in open-chest dogs. This study, however did not compare the temporal evolution of torsion in the open- and closed-chest preparations.

Buchalter et al. (1994) reported that torsion was greater in the canine posterior wall, while our results indicate that it was greater in the anterior wall and least in the posterior wall. The greater torsion in the anterior wall

is consistent with human studies (Buchalter et al., 1990; Lorenz et al., 2000). The discrepancy may be a result of the Buchalter et al. (1994) study examining only the torsion at a single time point, which may have missed the overall trend. Results from our canine model may translate to humans, as it has recently been reported that the magnitude and systolic time course of ventricular torsion were equivalent in mouse and humans, when normalized for heart rate and ventricular length (Henson et al., 2000).

Physiological Interpretation of the Results

The myocardial fibers in the LV vary in direction from the endocardium to the epicardium (Streeter et al., 1969), resulting in the fiber directions in the two layers



being nearly orthogonal. This anisotropy due to muscle fiber variation gives rise to ventricular torsion, with the apex moving counterclockwise when viewed from apex to base. This twist permits the endocardium to decrease its radius by a greater distance for a given amount of contraction, resulting in greater ejection. The untwisting of the LV during diastole is thought to aid in the filling process by releasing stored energy, resulting in a negative transmural pressure that initiates the rapid filling phase of diastole (Courtois et al., 1988; Nikolic et al., 1988; Robinson et al., 1986). Left ventricular untwist has been shown to occur before the relaxation of the ventricle (Beyar et al., 1989; Rademakers, 1992), and the rate of untwist has recently been shown to be independent of left atrial pressure (Dong et al., 2001).

Ectopic pacing has been shown to induce mechanical asynchrony (Wyman et al., 1999). It is possible that the asynchrony of contraction induced by pacing contributes to an asynchrony of relaxation, resulting in the massive overshoot of untwist that is consistently seen in the paced hearts.

It has been well established that pacing affects the rate of pressure change in the heart as well as the relaxation constant (Bedotto et al., 1990; Heyndrickx et al., 1988). However, we did not see any significant changes in pressure or dp/dt_{\min} across pacing protocols in this study. It is therefore unlikely that the changes in torsion resulting from pacing may be responsible for the decreased filling rate as seen by the reductions in dp/dt_{\min} .

Tagged MRI can be used to noninvasively evaluate the full-cycle, rotational mechanics of the paced heart. While other methods such as complementary spatial modulation of magnetization (CSPAMM) have been used to analyze the mechanics of the heart throughout the cardiac cycle (Stuber et al., 1999), this method provides a significantly higher signal-to-noise ratio without introducing subtraction artifacts. Asynchronous ventricular activation disrupts the normal physiological twist patterns simulated by RA pacing in both systole and diastole. Increasing the synchrony of contraction through Bi-V pacing (Wyman et al., 2002) does not change the temporal pattern of rotation found from pacing from the RVa site alone. It is clear that activation of the heart outside the normal sequence provided by the Purkinje network radically alters the normal pattern of LV torsion.

NOTATION

LV	Left ventricle
R_{\max}	Peak rotation

dp/dt_{\min}	Maximum decline in pressure during filling
RA	Right atrium
RVa	Apex of the right ventricle
Bi-V	Biventricular
$\theta_{\text{base}}, \theta_{\text{apex}}$	Rotation of the basal and apical slice, respectively
$\theta_{\text{apex}} - \theta_{\text{base}}$	Twist
$(\theta_{\text{apex}} - \theta_{\text{base}})/L$	Torsion
L	The distance from the center of the apical-most, short-axis slice to the center of the basal-most, short-axis slice
T_{\max}, T_{\min}	Maximum and minimum peak twists, respectively.

ACKNOWLEDGMENT

Supported in part by National Institutes of Health grant HL45683 (to E.R.M.).

REFERENCES

- Arts, T., Meerbaum, S., Reneman, R. S., Corday, E. (1984). Torsion of the left ventricle during the ejection phase in the intact dog. *Cardiovasc. Res.* 18:183–193.
- Axel, L., Dougherty, L. (1989). MR imaging of motion with spatial modulation of magnetization. *Radiology* 171:841–845.
- Badke, F. R., Boinay, P., Covell, J. W. (1980). Effects of ventricular pacing on regional left ventricular performance in the dog. *Am. J. Physiol.* 238: H858–H867.
- Bedotto, J. B., Grayburn, P. A., Black, W. H., Raya, T. E., McBride, W., Hsia, H. H., Eichhorn, E. J. (1990). Alterations in left ventricular relaxation during atrioventricular pacing in humans. *J. Am. Coll. Cardiol.* 15:658–664.
- Beyar, R., Yin, F. C., Hausknecht, M., Weisfeldt, M. L., Kass, D. A. (1989). Dependence of left ventricular twist-radial shortening relations on cardiac cycle phase. *Am. J. Physiol.* 257:H1119–H1126.
- Buchalter, M. B., Rademakers, F. E., Weiss, J. L., Rogers, W. J., Weisfeldt, M. L., Shapiro, E. P. (1994). Rotational deformation of the canine left ventricle measured by magnetic resonance tagging: effects of catecholamines, ischaemia, and pacing. *Cardiovasc. Res.* 28:629–635.
- Buchalter, M. B., Weiss, J. L., Rogers, W. J., Zerhouni, E. A., Weisfeldt, M. L., Beyar, R.,



- Shapiro, E. P. (1990). Noninvasive quantification of left ventricular rotational deformation in normal humans using magnetic resonance imaging myocardial tagging. *Circulation* 81:1236–1244.
- Courtois, M., Kovacs, S. J., Jr., Ludbrook, P. A. (1988). Transmitral pressure-flow velocity relation. Importance of regional pressure gradients in the left ventricle during diastole. *Circulation* 78:661–671.
- Dong, S. J., Hees, P. S., Siu, C. O., Weiss, J. L., Shapiro, E. P. (2001). MRI assessment of LV relaxation by untwisting rate: a new isovolumic phase measure of tau. *Am. J. Physiol. Heart Circ. Physiol.* 281:H2002–H2009.
- Eichhorn, E. J., Heesch, C. M., Risser, R. C., Marcoux, L., Hatfield, B. (1995). Predictors of systolic and diastolic improvement in patients with dilated cardiomyopathy treated with metoprolol. *J. Am. Coll. Cardiol.* 25:154–162.
- Gibbons-Kroeker, C. A., Tyberg, J. V., Beyar, R. (1995). Effects of load manipulations, heart rate, and contractility on left ventricular apical rotation. An experimental study in anesthetized dogs. *Circulation* 92:130–141.
- Guttman, M. A., Prince, J. L., McVeigh, E. R. (1994). Tag and contour detection in tagged MR images of the left ventricle. *IEEE T. Med. Imagrans.* 74–88.
- Guttman, M. A., Zerhouni, E. A., McVeigh, E. R. (1997). Analysis of cardiac function from MR images. *IEEE Comput. Graph. Appl.* 17:30–38.
- Henson, R. E., Song, S. K., Pastorek, J. S., Ackerman, J. J., Lorenz, C. H. (2000). Left ventricular torsion is equal in mice and humans. *Am. J. Physiol. Heart Circ. Physiol.* 278:H1117–H1123.
- Heyndrickx, G. R., Vantrimpont, P. J., Rousseau, M. F., Pouleur, H. (1988). Effects of asynchrony on myocardial relaxation at rest and during exercise in conscious dogs. *Am. J. Physiol.* 254:H817–H822.
- Ingels, N. B., Jr., Daughters, G. T., II, Stinson, E. B., Alderman, E. L. (1975). Measurement of midwall myocardial dynamics in intact man by radiography of surgically implanted markers. *Circulation* 52:859–867.
- Lorenz, C. H., Pastorek, J. S., Bundy, J. M. (2000). Delineation of normal human left ventricular twist throughout systole by tagged cine magnetic resonance imaging. *J. Cardiovasc. Magn. Reson.* 2:97–108.
- McVeigh, E. R. (1996). MRI of myocardial function: motion tracking techniques. *Magn. Reson. Imaging* 14:137–150.
- McVeigh, E. R., Zerhouni, E. A. (1991). Noninvasive measurement of transmural gradients in myocardial strain with MR imaging. *Radiology* 180:677–683.
- McVeigh, E. R., Atalar, E. (1992). Cardiac tagging with breath-hold cine MRI. *Magn. Reson. Med.* 28:318–327.
- McVeigh, E. R., Prinzen, F. W., Wyman, B. T., Tsitlik, J. E., Halperin, H. R., Hunter, W. C. (1998). Imaging asynchronous mechanical activation of the paced heart with tagged MRI. *Magn. Reson. Med.* 39(4):507–513.
- Nikolic, S., Yellin, E. L., Tamura, K., Vetter, H., Tamura, T., Meisner, J. S., Frater, R. W. (1988). Passive properties of canine left ventricle: diastolic stiffness and restoring forces. *Circ. Res.* 62:1210–1222.
- O'Dell, W. G., Moore, C. C., Hunter, W. C., Zerhouni, E. A., McVeigh, E. R. (1995). Three-dimensional myocardial deformations: calculation with displacement field fitting to tagged MR images. *Radiology* 195:829–835.
- Ohno, M., Cheng, C. P., Little, W. C. (1994). Mechanism of altered patterns of left ventricular filling during the development of congestive heart failure. *Circulation* 89:2241–2250.
- Rademakers, F. E., Buchalter, M. B., Rogers, W. J., Zerhouni, E. A., Weisfeldt, M. L., Weiss, J. L., Shapiro, E. P. (1992). Dissociation between left ventricular untwisting and filling. Accentuation by catecholamines. *Circulation* 85:1572–1581.
- Robinson, T. F., Factor, S. M., Sonnenblick, E. H. (1986). The heart as a suction pump. *Sci. Am.* 254:84–91.
- Streeter, D. D., Jr., Spotnitz, H. M., Patel, D. P., Ross, J., Jr., Sonnenblick, E. H. (1969). Fiber orientation in the canine left ventricle during diastole and systole. *Circ. Res.* 24:339–347.
- Stuber, M., Spiegel, M. A., Fischer, S. E., Scheidegger, M. B., Danias, P. G., Pedersen, E. M., Boesiger, P. (1999). Single breath-hold slice-following CSPAMM myocardial tagging. *Magma* 9:85–91.
- Tsitlik, J. E., Levin, H. E., McVeigh, E. R., Rogers, W., Perry, L., Halperin, H. (1992). Safe and reliable pacing in dogs during MRI in a 1.5 T magnet. In: Proceedings of the 13th Annual North American Society of Pacing and Electrophysiology; p. 561.
- Waldman, L. K., Fung, Y. C., Covell, J. W. (1985). Transmural myocardial deformation in the canine left ventricle. Normal in vivo three-dimensional finite strains. *Circ. Res.* 57:152–163.
- Wyman, B. T., Hunter, W. C., Prinzen, F. W., McVeigh, E. R. (1999). Mapping propagation of



mechanical activation in the paced heart with MRI tagging. *Am. J. Physiol.* 276:H881–H891.

Wyman, B. T., Hunter, W. C., Prinzen, F. W., Faris, O. P., McVeigh, E. R. (2002). Effects of single- and biventricular pacing on temporal and spatial dynamics of ventricular contraction. *Am. J. Physiol. Heart Circ. Physiol.* 282:H372–H379.

Yun, K. L., Niczyporuk, M. A., Daughters, G. T., II, Ingels, N. B., Jr., Stinson, E. B., Alderman, E. L., Hansen, D. E., Miller, D. C. (1991). Alterations in left ventricular diastolic twist mechanics during acute human cardiac allograft rejection. *Circulation* 83:962–973.

Received January 2, 2002

Accepted June 29, 2003

